Large-Scale, Decelerating, Relativistic X-ray Jets from the Microquasar XTE J1550–564

S. Corbel,[1]* R. P. Fender,[2] A. K. Tzioumis,[3] J. A. Tomsick,[4] J. A. Orosz,[5] J. M. Miller,[6] R. Wijnands,[6] P. Kaaret[7]

We have detected, at x-ray and radio wavelengths, large-scale moving jets from the microquasar XTE J1550–564. Plasma ejected from near the black hole traveled at relativistic velocities for at least 4 years. We present direct evidence for gradual deceleration in a relativistic jet. The broadband spectrum of the jets is consistent with synchrotron emission from high-energy (up to 10 tera–electron volts) particles that were accelerated in the shock waves formed within the relativistic ejecta or by the interaction of the jets with the interstellar medium. XTE J1550–564 offers a rare opportunity to study the dynamical evolution of relativistic jets on time scales inaccessible for active galactic nuclei jets, with implications for our understanding of relativistic jets from Galactic x-ray binaries and active galactic nuclei.

Collimated relativistic jets produced by active galactic nuclei (*1*) (AGN) and by accretion-powered stellar compact objects in sources called microquasars (*2*) are commonly observed at radio wavelengths. Such jets are produced close to black holes (supermassive ones in AGN and stellar-mass ones in microquasars) and may help probe the dynamics of matter being accreted in intense gravitational fields. The unprecedented subarc second resolution of the Chandra x-ray observatory has recently allowed the detection of x-ray jets in many AGN. Whereas the radio emission of AGN jets is thought to originate from synchrotron emission, the nature of the x-ray emission is still under debate; but synchrotron or inverse Compton radiation is likely involved (*3*). Jets produced by Galactic black holes such as XTE J1550–564 should evolve much more rapidly than AGN jets and, therefore, could provide insights into the dynamical evolution of relativistic outflows and also into the processes of particle acceleration. Here, we present the detection of large-scale, moving, relativistic jets ejected from a Galactic black hole binary.

The x-ray transient XTE J1550–564 (Galactic longitude and latitude $l = 325.88°$, $b = -1.83°$) was discovered by the All-Sky Monitor (ASM) aboard the Rossi X-ray Timing Explorer (RXTE) on 7 September 1998 (*4*). Shortly afterward, a strong and brief (about 1 day) x-ray flare was observed on 20 September 1998 (*5*, *6*), and radio jets with apparent superluminal velocities ($>2\ c$, where c is the speed of light) were observed beginning 24 September 1998 (*7*). Subsequent optical observations showed that the dynamical mass of the compact object is 10.5 ± 1.0 stellar masses, indicating that the compact object in XTE J1550–564 is a black hole; revealed the binary companion to be a low-mass star; and led to a distance estimate of about 5.3 kpc (*8*).

After the reappearance of x-ray emission from XTE J1550–564 in early 2002 (*9*), we initiated a series of radio observations with the Australia Telescope Compact Array (ATCA). Observations on 16 January 2002 showed renewed activity at radio wavelengths from the XTE J1550–564 black hole binary (*10*). These observations also revealed a previously unknown radio source ~22 arc sec to the west of the black hole binary. ATCA observations performed on 29 January 2002 (Fig. 1), in an array configuration allowing higher spatial resolution imaging, showed that the western source had a possible extension pointed toward XTE J1550–564. The position angle of this radio source relative to XTE J1550–564 was $-85.8° \pm 1.0°$, which is consistent with the position angle [$-86.1° \pm 0.8°$ (*11*)] of the western component of the superluminal jet observed during the September 1998 radio flare with long baseline interferometry (*7*).

Prompted by the detection of the western source along the axis of the jet from XTE J1550–564, we searched Chandra archival data taken in 2000 for x-ray sources located along the jet axis of XTE J1550–564. The field of view of XTE J1550–564 was imaged by Chandra on 9 June, 21 August, and 11 September of 2000. Examination of the 0.3- to 8-keV images (Fig. 2) revealed an x-ray source ~23 arc sec to the east of XTE J1550–564 at a position angle of $93.8° \pm 0.9°$ from XTE J1550–564, lying along the axis of the eastern components of the radio superluminal jets (*7*) [at a position angle of $93.9° \pm 0.8°$ (*11*)]. The angular separation between this eastern source and XTE J1550–564 increased from 21.3 ± 0.5 arc sec on 9 June 2000 to 23.4 ± 0.5 arc sec on 11 September 2000, implying that the eastern source moved with an average proper motion of 21.2 ± 7.2 milli–arc sec (mas) day^{-1} between these two observations. Thus, we were able to obtain an x-ray jet proper-motion measurement, something not previously done for any accretion-powered Galactic or extragalactic source. Our radio observations (Fig. 1), performed with ATCA between April 2000 and February 2001, showed a weak, decaying, and moving radio source consistent with the position of the eastern x-ray source. It was not detected in February 2002 (Fig. 1) with a 3σ upper limit of 0.18 mJy ($1\ \text{Jy} = 10^{-26}\ \text{W m}^{-2}\ \text{Hz}^{-1}$) at 3.5 cm.

With the detection of the western radio source in early 2002, we obtained a 30-ks Chandra observation on 11 March 2002. In the resulting 0.3- to 8-keV image (Fig. 2), three sources were detected along the axis of the jet: the x-ray binary XTE J1550–564, an extended x-ray source at the position of the western radio source, and a faint source 29.0 ± 0.5 arc sec east of XTE J1550–564. This weak x-ray source was the eastern source that had smoothly decayed and moved by 5.7 ± 0.7 arc sec since September 2000. The eastern source was active during a period of at least 2 years (from April 2000 to March 2002).

The most remarkable feature of this Chandra observation is the x-ray emission associated with the western radio source. Both the radio and x-ray emissions of the western source appeared extended toward XTE J1550–564, and the morphology matched well between the two wavelengths. Most (70%) of the x-ray emission was concentrated in the leading peak, which has a full width at half maximum (FWHM) of 1.2 arc sec. A trailing tail, pointed back toward XTE J1550–564, gave a full width at 10% of maximum intensity of 5 arc sec.

The alignment of the eastern and western sources with the axis of the jet observed on 24 September 1998 (*7*), as well as the proper motion of the eastern source, imply that both

[1]Université Paris VII and Service d'Astrophysique, Commissariat à l'Energie Atomique CE-Saclay, 91191 Gif sur Yvette, France. [2]Astronomical Institute Anton Pannekoek, University of Amsterdam, and Center for High Energy Astrophysics, Kruislaan 403, 1098 SJ Amsterdam, Netherlands. [3]Australia Telescope National Facility, Commonwealth Scientific and Industrial Research Organization (CSIRO), Post Office Box 76, Epping NSW 1710, Australia. [4]Center for Astrophysics and Space Sciences, University of California at San Diego, MS 0424, La Jolla, CA 92093, USA. [5]Astronomical Institute, Utrecht University, Postbus 80000, 3508 TA Utrecht, Netherlands. [6]Center for Space Research, Massachusetts Institute of Technology, NE80-6055, 77 Massachusetts Avenue, Cambridge, MA 02139–4307, USA. [7]Harvard-Smithsonian Center for Astrophysics, 60 Garden Street, Cambridge, MA 02138, USA.

*To whom correspondence should be addressed. E-mail: corbel@discovery.saclay.cea.fr

sources are related to the jets of XTE J1550–564. In addition, both sources are likely to be connected with the apparently superluminal ejecta from the brief and intense flare of 20 September 1998 (*7*). Indeed, large-scale ejections of relativistic plasma (from XTE J1550–564) have been observed and resolved only during this occasion; the radio emission detected at other epochs has been associated with the compact jet of the low-hard x-ray spectral state (*12*). Also, the RXTE-ASM has not detected any other x-ray flares similar to the large flare of 20 September 1998 in subsequent monitoring. The fact that the eastern source apparently moves faster than the western source is consistent with the interpretation in which the eastern source constitutes the jet that is pointing toward Earth (the approaching jet) and the western source constitutes the receding jet.

With the positions of the eastern (and approaching) jet on 9 June 2000 and that of the western (and receding) jet on 16 January 2002, we find average proper motions of 32.9 ± 0.7 mas day^{-1} and 18.3 ± 0.7 mas day^{-1}, respectively. At a distance of 5.3 kpc (*8*), this corresponds to average apparent velocities on the plane of the sky of 1.0 *c* and 0.6 *c* for the eastern and western jets, respectively. The proper motion of 21.2 ± 7.2 mas day^{-1} measured by Chandra for the eastern jet between 9 June 2000 and 11 September 2000 is significantly smaller than its corresponding average proper motion, which indicates that the ejecta decelerated after the ejection. This is confirmed by the Chandra detection of the eastern jet in March 2002, implying an average proper motion of 10.4 ± 0.9 mas day^{-1} between 11 September 2000 and 11 March 2002. The relativistic plasma was originally ejected at greater velocities, because the relative velocity was initially greater than 2 *c* [the initial proper motion was greater than 57 mas day^{-1} for the approaching jet (*7*)]. These observations provide direct evidence for gradual deceleration of relativistic materials in a jet. Previous observations of other microquasars are consistent with purely ballistic motions [for example (*2*, *13*)], except for the system called XTE J1748–288, where after ballistic ejections, the jet was observed to stop suddenly, presumably after a collision with environmental material (*14*, *15*).

The eastern and western jets have been detected up to angular separations from XTE J1550–564 of 29 and 23 arc sec, respectively, which correspond to projected physical separations of 0.75 and 0.59 pc, respectively, for a distance of 5.3 kpc (*8*). These are large distances for moving relativistic ejecta [in GRS 1915+105, the ejecta have been observed to travel up to a projected distance of 0.08 pc and on a maximum time scale of 4 months (*2*)]. Persistent large-scale (1 to 3 pc) jets have previously been observed only at radio wavelengths, for example, 1E 1740.7–2942 and GRS 1758–258 (*16*, *17*), but without indication of associated moving ejecta. Our observations reveal that the relativistic ejecta of a Galactic black hole have been able to travel over parsec-scale distances at relativistic velocities during several years. An important aspect of our study is that it provides direct evidence for a large-scale, moving x-ray jet from a black hole (Galactic or in AGN).

SS 433 is the only other x-ray binary for which large-scale (up to ~40 arc min, i.e., several tens of parsecs), nonthermal x-ray emission has been previously observed, probably associated with interactions of the jets with the interstellar medium (ISM) (*18*–*22*). The helical pattern observed in the lobes at radio wavelengths indicates a connection between the lobes and the corkscrew pattern associated with plasma ejection close to (on an arc sec scale) the core of the SS 433/W50 system (*23*). However, relativistic motion at large scales has not been observed in SS 433. We note that thermal x-ray emission arising from moving relativistic ejecta, but only out to ~0.05 pc from the compact object, has been reported in SS 433 (*24*, *25*).

Our results demonstrate that the emission from relativistic ejecta of Galactic black holes can be observed at wavelengths extending up to x-rays. Future sensitive, high-resolution observations of other Galactic black hole jets in the infrared (*26*), optical, and x-ray bands may reveal that broadband emission from relativistic ejecta of Galactic black holes is more common than previously thought and may offer an exciting way to probe the physics of the jets. AGN jets, which were previously detected at radio and optical wavelengths, are now known, with the advent of the Chandra observatory, to often produce x-rays. Whereas the radio emission of AGN jets is thought to originate from synchrotron emission, the nature of the x-ray emission has

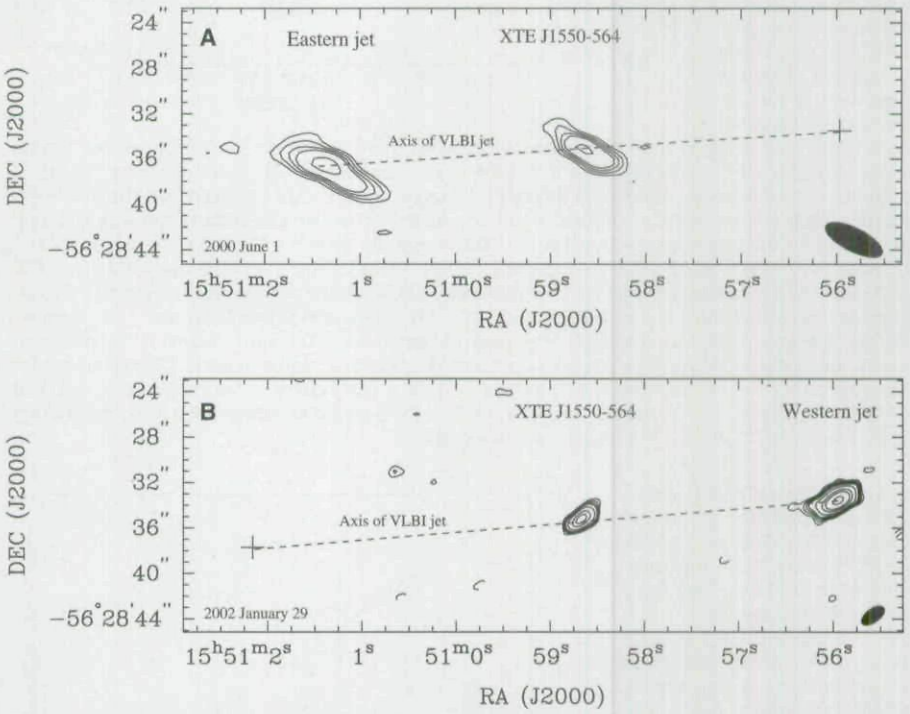

Fig. 1. Uniform weighted maps of the field of view around the black hole candidate XTE J1550–564 on 1 June 2000 (A) and 29 January 2002 (B) showing the radio counterpart to the eastern and western jets (when detected). RA, right ascension; DEC, declination. The stationary black hole binary XTE J1550–564 is at the center of the images and has a radio spectrum typical of the self-absorbed compact jet (*33*, *34*) that is observed during the x-ray low-hard spectral state (*12*). (**A**) 1 June 2000 map at 4800 MHz (6 cm). The position of the eastern radio jet is α(J2000) = 15h 51m 01s.30 and δ(J2000) = –56°28′ 36.9″, with a total uncertainty of 0.3 arc sec; that is, at a position angle of 93.8° ± 0.9° from XTE J1550–564. The synthesized beam (in the lower right corner) is 5.5 × 2.1 arc sec, with the major axis in a position angle of 63.1°. The peak brightness in the image is 1.1 mJy per beam. Contours are plotted at –3, 3, 4, 5, 6, and 9 times the root mean squared (rms) noise equal to 0.1 mJy per beam. The cross marks the position of the western jet as measured on 29 January 2002. (**B**) 29 January 2002 map at 8640 MHz (3.5 cm). The position of the western radio jet is α(J2000) = 15h 50m 55s.94 and δ(J2000) = –56°28′ 33.5″, with a total uncertainty of 0.3 arc sec. The synthesized beam is 2.4 × 1.3 arc sec with the major axis in a position angle of –54.6°. The peak brightness in the image is 1.79 mJy per beam. Contours are plotted at –3, 3, 4, 5, 6, 9, 15, 20, and 30 times the rms noise equal to 0.05 mJy per beam. The cross marks the position of the eastern jet as measured on 11 March 2002 during the Chandra observation.

not always been clearly identified. Although it is thought to be nonthermal, it is not always known whether synchrotron or inverse Compton radiation predominates for a particular object (*3*, *27*–*29*).

The nature of the physical mechanism producing the emission from the relativistic jets of XTE J1550–564 can be understood by looking at the broadband spectrum, for example, for the western jet on 11 March 2002 (Fig. 3). The position and morphology of the radio and x-ray counterparts of the western jet are consistent with each other (Figs. 1 and 2), and the spectral energy distribution is consistent with a single power law (of spectral index -0.660 ± 0.005). These facts favor a scenario in which the broadband emission from the jets is synchrotron emission from high-energy particles. Similar conclusions could be drawn for the eastern jet in 2000, because the overall radio flux was also consistent with an extrapolation of the x-ray spectrum with a spectral index of -0.6. The detection of x-ray synchrotron emission would imply a large Lorentz factor, on the order of 2×10^7 (corresponding to an energy of ~10 TeV), for the x-ray–emitting electrons (under the equipartition assumption giving a magnetic field of ~0.3 mG).

Acceleration in a shock wave is the most likely origin for the very high energies required. Shock waves could be produced by internal instabilities (*30*) or by varying flow speeds within the jet, as has been proposed to occur in some models of gamma-ray bursts or AGN (*31*, *32*). If several relativistic plasmoids were ejected around 24 September 1998 (*7*) and their velocities were slightly different, then it would have taken several months (maybe years) for them to collide. Such a collision would have produced shock waves, particle acceleration, and the brightening of the jets.

A more plausible alternative is that the shock waves are produced when the jet material, moving with bulk relativistic speed, interacts with the ISM (producing an external shock). In fact, the gradual deceleration we observed for the eastern jet would be easily explained by such interactions. Inhomogeneities in the ISM could also be at the origin of the brightening of the eastern and western jet at different epochs. The origin of the western jet is less clear because no proper motion has been observed yet. Continuous observations of XTE J1550–564 will show whether or not the western jet is still moving and, together with high spatial resolution observations and broadband spectra, will be important in deciding between the models (internal or external shocks). Also, regular observation of the jets of XTE J1550–564 would map the propagation of the shocks and allow estimation of the energy dissipated in the jets when decelerating in the ISM. XTE J1550–564 offers a unique opportunity to study the dynamical evolution of relativistic jets on time scales inaccessible for AGN jets and has implications not only for the study of jets from Galactic x-ray binaries but also for our understanding of relativistic jets from AGN.

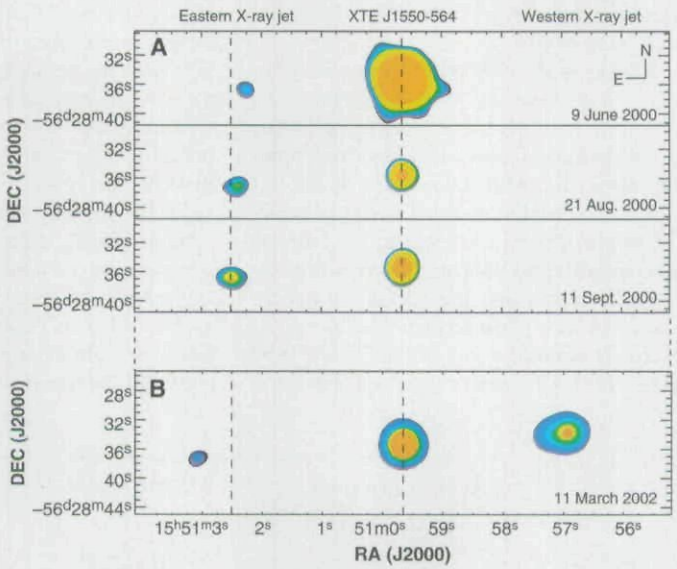

Fig. 2. Chandra 0.3- to 8-keV images (using the Advanced Charged-Coupled Device Imaging Spectrometer spectroscopy array ACIS-S), which show the black hole binary XTE J1550–564 (center), the approaching eastern x-ray jet (left), and the receding western x-ray jet (right). The observations are ordered chronologically from top to bottom, and each image is labeled with the observation date. These filled contour plots have been produced by convolving the original Chandra image with a two-dimensional Gaussian with a width of 2 pixels in both directions. In 2000 (**A**), there are 11 contours between the lowest contour of 1.33×10^{-3} count s^{-1} $pixel^{-1}$ and the highest contour of 8.16×10^{-3} count s^{-1} $pixel^{-1}$. The same contour levels are used in all three 2000 images, but it should be noted that the flux levels for 9 June 2000 are not directly comparable to those for the other two observations because a grating was inserted for the 9 June observation. For the 2002 image (**B**), there are 11 contours between 0.33×10^{-3} count s^{-1} $pixel^{-1}$ and 8.16×10^{-3} count s^{-1} $pixel^{-1}$. The dashed lines mark the positions of XTE J1550–564 and the eastern x-ray jet on 11 September 2000, when the sources were separated by 23".4. The proper motion of the x-ray jet is 21.2 ± 7.2 mas day^{-1} between 9 June 2000 and 11 September 2000 and averages 10.4 ± 0.9 mas day^{-1} between 11 September 2000 and 11 March 2002, indicating deceleration of the jet. Assuming a power-law spectral shape with a photon index of 1.7 and interstellar absorption of $N_H = 9 \times 10^{21}$ cm^{-2}, a count rate of 1.33×10^{-3} count s^{-1} corresponds to a flux of 7.71×10^{-14} erg cm^{-2} s^{-1} in the 0.3- to 8-keV band for the 9 June 2000 observation (with the grating) and to 1.66×10^{-14} erg cm^{-2} s^{-1} for other observations.

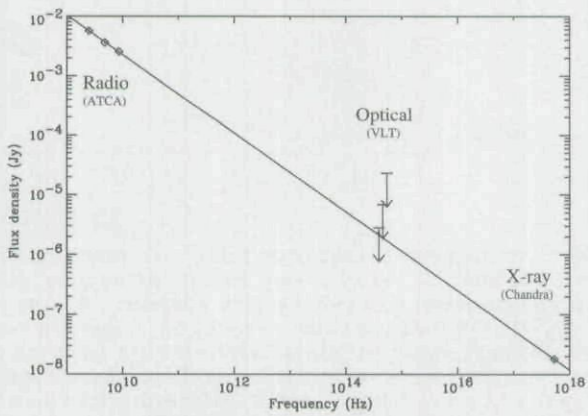

Fig. 3. The spectral energy distribution of the western jet around 11 March 2002. The radio points near 10^{10} Hz are ACTA measurements from 6 March. The radio flux densities were 5.7 ± 0.3, 3.60 ± 0.08, and 2.55 ± 0.07 mJy at 2496, 4800, and 8640 MHz, respectively, giving a spectral index of -0.63 ± 0.05 in the radio range. The x-ray measurement near 5×10^{17} Hz is the Chandra measurement from 11 March. X-ray spectral fitting of the Chandra data for the western source, assuming a power-law form with interstellar absorption fixed to the total Galactic atomic hydrogen column density ($N_H = 9.0 \times 10^{21}$ cm^{-2}), gives a spectral index of -0.70 ± 0.15 (90% confidence level). The spectrum may be somewhat steeper if there is additional absorption near the source. The unabsorbed 0.3- to 8-keV flux is 3.8×10^{-13} ergs cm^{-2} s^{-1} (i.e., 18 nJy at 2.2 keV). The optical upper limits (99% confidence level) in between are derived from deep observations carried out with the 8.2-m unit 3 telescope at the ESO, Paranal. The source was observed with the FORS1 instrument in the Bessel *V* and *R* filters on 10 March, with limiting magnitudes for point sources of 25.2 and 25.5 mag., respectively, and on 18 March with FORS1 and the Bessel *I* filter, with a limiting magnitude for point sources of 25.5 mag. We assumed an optical extinction of $A_V = 4.75$ mag (*8*). The broadband spectral energy distribution is consistent with a single power law of spectral index of -0.660 ± 0.005.

References and Notes

1. A. H. Bridle, R. A. Perley, *Annu. Rev. Astron. Astrophys.* **22**, 319 (1984).
2. I. F. Mirabel, L. F. Rodríguez, *Annu. Rev. Astron. Astrophys.* **37**, 409 (1999).
3. D. E. Harris, H. Krawczynski, *Astrophys. J.* **565**, 244 (2002).
4. D. A. Smith, *Int. Astron. Union Circ. No. 7008* (1998).
5. G. J. Sobczak *et al.*, *Astrophys. J.* **544**, 993 (2000).

6. J. Homan *et al.*, *Astrophys. J. Suppl. Ser.* **132**, 377 (2001).
7. D. Hannikainen *et al.*, *Astrophys. Space Sci. Rev.* **276**, 45 (2001).
8. J. A. Orosz *et al.*, *Astrophys. J.* **568**, 845 (2002).
9. J. Swank, E. Smith, C. Markwardt, *Int. Astron. Union Circ. No. 7792* (2002).
10. S. Corbel, R. P. Fender, A. K. Tzioumis, *Int. Astron. Union Circ. No. 7795* (2002).
11. D. Hannikainen, personal communication.
12. S. Corbel *et al.*, *Astrophys. J.* **554**, 43 (2001).
13. R. P. Fender *et al.*, *Mon. Not. R. Astron. Soc.* **304**, 865 (1999).
14. T. Kotani *et al.*, *Astrophys. J.* **543**, L133 (2000).
15. M. Rupen, personal communication.
16. I. F. Mirabel, L. F. Rodríguez, B. Cordier, J. Paul, F. A. Lebrun, *Nature* **358**, 215 (1992).
17. L. F. Rodríguez, I. F. Mirabel, J. Martí, *Astrophys. J.* **401**, L15 (1992).
18. F. Seward, J. Grindlay, E. Seaquist, W. Gilmore, *Nature* **287**, 806 (1980).
19. M. G. Watson, R. Willingale, J. E. Grindlay, F. D. Seward, *Astrophys. J.* **273**, 688 (1983).
20. W. Brinkmann, B. Aschenbach, N. Kawai, *Astron. Astrophys.* **312**, 306 (1996).
21. S. Safi-Harb, H. Oegelman, *Astrophys. J.* **483**, 868 (1997).
22. S. Safi-Harb, R. Petre, *Astrophys. J.* **512**, 784 (1999).
23. G. M. Dubner, M. Holdaway, W. M. Goss, I. F. Mirabel, *Astron. J.* **116**, 1842 (1998).
24. H. L. Marshall, C. R. Canizares, N. S. Schulz, *Astrophys. J.* **564**, 941 (2002).
25. S. Migliari, R. P. Fender, M. Méndez, *Science* **297**, 1673 (2002).
26. B. J. Sams, A. Eckart, R. Sunyaev, *Nature* **382**, 47 (1996).
27. A. S. Wilson, A. J. Young, P. L. Shopbell, *Astrophys. J.* **547**, 740 (2001).
28. R. M. Sambruna *et al.*, *Astrophys. J.* **549**, L161 (2001).
29. R. M. Sambruna *et al.*, *Astrophys. J.* **571**, 206 (2002).
30. P. E. Hardee, *Astrophys. J.* **533**, 176 (2000).
31. M. J. Rees, P. Meszaros, *Astrophys. J.* **430**, L93 (1994).
32. C. R. Kaiser, R. Sunyaev, H. C. Spruit, *Astron. Astrophys.* **356**, 975 (2000).
33. R. M. Hjellming, K. J. Johnston, *Astrophys. J.* **328**, 600 (1988).
34. R. P. Fender, *Mon. Not. R. Astron. Soc.* **322**, 31 (2001).

35. S.C. and J.A.T. acknowledge useful conversations with A. Celotti, S. Heinz, and V. Dhawan. P.K. acknowledges useful discussions with H. Falcke and D. Harris. S.C. thanks C. Bailyn, S. Chaty, D. Hannikainen, and D. Hunstead for providing information before publication; F. Mirabel for a careful reading of this manuscript; and R. Ekers, D. McConnell, R. Norris, B. Sault, and the ATCA Time Allocating Committee for allowing the radio observations. We thank H. Tananbaum for granting Director's Discretionary Time for the Chandra observations and J. Nichols for rapid processing of the data. We have made use of observations performed with the European Southern Observatory (ESO) Melipal Telescope at the Paranal Observatory under Director's Discretionary Time program 268.D-5771. The Australia Telescope is funded by the Commonwealth of Australia for operation as a National Facility managed by CSIRO.

8 July 2002; accepted 26 August 2002

Condensation of Semiconductor Microcavity Exciton Polaritons

Hui Deng,[1]* Gregor Weihs,[1,2] Charles Santori,[1] Jacqueline Bloch,[3] Yoshihisa Yamamoto[1,4]

A phase transition from a classical thermal mixed state to a quantum-mechanical pure state of exciton polaritons is observed in a GaAs multiple quantum-well microcavity from the decrease of the second-order coherence function. Supporting evidence is obtained from the observation of a nonlinear threshold behavior in the pump-intensity dependence of the emission, a polariton-like dispersion relation above threshold, and a decrease of the relaxation time into the lower polariton state. The condensation of microcavity exciton polaritons is confirmed.

The search for the macroscopic quantum coherence formed in a degenerate Bose gas drives the worldwide work on atom Bose-Einstein condensation (BEC). Though the observed first order coherence of atoms is a direct manifestation of the wave nature of matter, only second-order and higher-order coherence functions can distinguish quantum-mechanical pure states from a classical thermal mixed state (*1*). In quantum optics, quantum phase transitions have been studied extensively for lasers and parametric oscillators via the second order coherence function. For atomic BECs, the second- and third-order coherence functions have been measured indirectly in the spatial domain (*2*, *3*) but not in the time domain. Semiconductor exciton polaritons constitute another promising system to explore the physics of degenerate Bose gases, but in a stronger interaction regime (*4*, *5*). However, conclusive evidence of condensation of excitons or polaritons has been elusive. We have obtained evidence for the formation of macroscopic quantum coherence by measuring the time domain of second-order coherence function $g^{(2)}(\tau)$ of the light emitted from the polaritons

$$g^2(\tau) = \frac{\langle \hat{E}^{(-)}(t)\hat{E}^{(-)}(t+\tau)\hat{E}^{(+)}(t+\tau)\hat{E}^{(+)}(t)\rangle}{\langle \hat{E}^{(-)}(t)\hat{E}^{(+)}(t)\rangle^2} \quad (1)$$

where $\hat{E}^{(-)}(t)$ and $\hat{E}^{(+)}(t)$ are the negative and positive frequency parts of the electric field operator at time t, respectively (*1*).

When the optical field of a semiconductor microcavity strongly couples to the heavy-hole excitons in embedded quantum wells (QWs) (Fig. 1A), new normal modes are formed, the lower polariton (LP) and the upper polariton (UP) (*6*). The coupling strength of the interband dipole moment to the cavity optical mode determines the splitting between the UP and LP energies. The confinement of the excitons in a QW lifts the degeneracy of the heavy-hole and light-hole excitons, so that the UP and the LP are only twofold degenerate by their spins. With integer total spin, QW excitons and cavity polaritons behave as interacting bosons in the low-density regime. The exchange interaction between the excitons' fermionic constituents, electrons and holes, introduces a repulsive interaction between excitons with identical spins (*4*, *5*, *7*, *8*). This weak repulsive interaction is indispensable for the formation of exciton or polariton BECs.

In the search for polariton condensation effects, a nonlinear emission has been observed in exciton-polariton systems (*9*–*11*), but the mechanism leading to the observed nonlinearity was not clarified. Pump-probe experiments (*12*, *13*) provided evidence of the bosonic final-state stimulation and the amplification of polaritons by polariton-polariton scattering, which is also the mechanism for creating the macroscopic polariton condensation in the work presented here. In our experiments, excitons with a large transverse momentum are initially created by optical pumping. They relax by polariton-polariton scattering (through the exciton component of the wave function) and cool subsequently by phonon emission, thereby losing the coherence inherited from the pump wave and forming a real exciton-polariton population with a quasi-thermal distribution (Fig. 1B). Due to the slow phonon emission rate and fast radiative decay rate in the region of small in-plane wavenumber $k_{\|}$ region, most of the injected excitons radiatively decay before they relax to the bottom of the LP branch (the $k_{\|} = 0$ LP state). However, it is expected that above a critical pump intensity, when the LP population per mode around $k_{\|} = 0$ approaches one, the elastic scattering of two LPs into the $k_{\|} = 0$ LP and a higher-energy LP is considerably enhanced due to bosonic final-state stimulation. This stimulated LP-LP scattering is a phase coherent process, analogous to the phase coherent stimulated emission in a laser. Consequently, a macroscopic coherent population can quickly build up in the $k_{\|} = 0$ LP state, forming a condensate.

[1]Quantum Entanglement Project, ICORP, JST, Edward L. Ginzton Laboratory, Stanford University, Stanford, CA 94305, USA. [2]Institut für Experimentalphysik, Universität Wien, Vienna, Austria. [3]LPN/CNRS, Route de Nozay, 91460, Marcoussis, France. [4]NTT Basic Research Laboratories, Astugishi, Kanagawa, Japan.

*To whom correspondence should be addressed. E-mail: dhui@stanford.edu